Review of liquid-crystal phase transitions with quenched random disorder

Germano S. Iannacchione

Department of Physics, Worcester Polytechnic Institute,

Worcester, Massachusetts 01609, USA

(Dated: May 5, 2003)

Abstract

Recent experimental and theoretical efforts have focused on using liquid-crystal systems as a test bed for understanding the statistical mechanics of quenched random disorder. In particular, the weakly first-order isotropic to nematic (I-N) and the second-order nematic to smectic-A (N-SmA) phase transitions have been intensely studied under two, topologically distinct configurations: (I) confined within a porous media as a function of pore size or (II) perturbed by an imbedded gel as a function of solids density. Thermodynamically singular phase behavior appears to be preserved in an experimentally accessible range of physical parameters governing both I and II. This work reviews the observed transitional behavior of the I-N and N-SmA phase transitions as a function of quenched random disorder given by these two configurations. The results to date have revealed a rich variety of effects, confirming some theoretical models, challenging others, all the while displaying ever new phenomena with relevance to a wide range of issues in complex fluids.

PACS numbers: 64.70.Md, 61.30.Eb, 61.10.-i

I. INTRODUCTION

Liquid-crystals (LC) are a class of materials exhibiting thermodynamically stable but only partially ordered phases. Each mesophase is described by its own order parameter, such as a second rank tensor for orientational order (nematic phase) or a two-component vector for the one-dimensional translational order (smectic phase). In addition, transitions between mesophases involve the breaking of continuous symmetries as well as a variety of universality classes. Therefore, many fundamental ideas of the modern theory of phase transitions and critical phenomena have been tested in LC systems. Although there remains some important outstanding questions, our understanding of bulk phase transitional behavior is largely a solved problem and a triumph of statistical mechanics.

The study of the effect of quenched random disorder (QRD) on phase transitional behavior remains an attractive area of research due to the broad implications outside the laboratory. The underlying physics has applications ranging from unique assemblies of complex fluids to doped semiconductors. Many systems have been the focus of both theoretical and experimental studies. The experimental efforts have concentrated on idealized model systems in the hopes of isolating the essential features of quenched random disorder. They include the still enigmatic superfluid transition of ^{4}He in aerogels and controlled porous glasses, the superfluid transition and phase separation of ^{4}He-^{3}He mixtures in silica aerogels [1], and doped magnet systems [2]. Relatively recent efforts with liquid-crystal (LC) – silica composites (using either aerogels or aerosils) [3–9] have demonstrated that these are especially interesting model systems. Vycor-like controlled porous glasses have also been used to study liquid-crystals [10–12] but there are still some important questions as to the nature of the disorder. Liquid-crystals are of particular importance as a way to access "soft" (elastically weak) phases of continuous symmetry, which are directly coupled to surfaces and external fields.

The general consensus is that the physics of QRD in liquid crystals is essentially contained by a random-field approach [13]. For second-order phase transitions, recent theoretical efforts predict that an Ising system with quenched random fields will move towards a new random-field Ising (RFI) fixed point with increasing disorder. However, a random-field XY (RFXY) system has no new fixed point that is stable. Here, with increasing strength of the disordering random field, an RFXY system still has flows toward the XY fixed

point until long-range order is destroyed [13]. Thus one expects, in general, that a 3D-XY system subject to random-field perturbations has no true long-range order (LRO). A detailed theoretical study of QRD effects on smectic ordering in liquid crystals [14] concludes that arbitrarily small amounts of QRD destroy even quasi-LRO and hence no true smectic phase exists since the smectic correlation length remains finite for all strengths of disorder and all temperatures. This theoretical conclusion is in agreement with x-ray studies of octylcyanobiphenyl (8CB)+aerosil dispersions [9, 15] as well as 8CB+aerogel [5, 16]. These x-ray studies reveal a finite smectic correlation length for all temperatures and densities of silica. However, for aerosil systems, the director and smectic correlation lengths are quite large and smectic thermal fluctuations still exist above a pseudo-nematic to smectic-A transition at T^* (close to but below T^o_{NA} for pure 8CB). These smectic fluctuations are expected to remain in the XY universality class but also show crossover behavior from Gaussian tricritical (TC) to 3D-XY with increasing strength of disorder [15].

First-order transitions with QRD have additional considerations than continuous transitions due to the possibility of two-phase coexistence (hence interfaces between ordered and disordered regions), intrinsically finite correlation length at the transition, and hysteresis effects. This has made the experimental and theoretical studies of quenched random disorder effects at first-order transitions much more challenging. Although the random-field model is the same starting point, first-order transitions have the added complication of an energy penalty for the formation of interfaces between coexisting phases [17]. In this view, the QRD effect is as a random-field in each domain randomly shifting each domains transition temperature thus smearing the overall transition. However, nematics are very "soft" materials, and their elasticity can play an important role. A recent theoretical study, applied renormalization group analysis to the ordering of nematics with quenched random disorder concluded that such systems belong to the Random-Anisotropy (RA) Heisenberg class [18]. The observed suppression of the latent-heat of the first-order transition to nematic order with increasing QRD for 8CB+aerogel and other rigidly confined porous systems appears to be consistent with the random transition temperature model [17] but the observed behavior for 8CB+aerosil is not and is perhaps more closely related to the RA-Heisenberg model [18].

In the above discussion, there are three relevant length scales to consider: the disorder correlation length d_S (the correlation length of the random surfaces), the mean-open length l_o (the correlation size of the open space), and the correlation length of the ordering phase

ξ. For a random-field system to be applicable, ξ may be equal to or larger than l_o depending on the extent of finite-size effects but d_S must be smaller than either in order for the average orientation of the effective field to be zero (although the average of the RF squared is not). For controlled porous glasses, the presence of pores suggests that a circumference exists that is a measure of d_S and larger than the mean-open length (diameter) by approximately a factor of π. In this case, both second and first-order phase transitions can be understood by a *single-pore* model [10, 11] where the observed behavior is the result of the average of a random distribution of individual pores.

In all fluid systems studied to date as models of QRD effects, including the liquid-crystal system mentioned above, the random perturbations are introduced via the embedding of a random (gel-like) solid structure into the phase ordering material or by the explicit confinement to a porous structure. An open question remains as to the connection between the concentration and randomness of such solid inclusions and the strength of the random disordering field. Also, the identification of QRD is complicated by finite-size effects which could, in principle, play a dominant role in such systems. In simple finite-size scaling (FSS), where the confining surfaces play no interactive role, the *bulk* critical correlation fluctuations are cut off at a length dictated by the distance between surfaces, which corresponds to a minimum reduced temperature where the transition is "truncated." However, when the surfaces are arranged in a random manner with high void connectivity in order to introduce QRD, the distance between surfaces no longer acts as an upper length scale in the system, and changes in the transition's critical behavior may also occur. Given the absence of LRO in such perturbed systems, the required characterization of the critical behavior may not be possible. In spite of this, if a critical power-law analysis of the transition heat capacity data is available, then, through two-scale universality, the critical behavior of the correlation length for $T > T^*$ may be estimated and compared with direct measurements. Finally, if the introduced random surfaces have in addition the freedom of an elastic response, then coupling between the gel and host elasticities can occur. This latter effect has only begun to be explored theoretically [19–21].

Given the myriad of effects possible with LC+QRD, the focus of this work is to review thermodynamic results for the same LC, octylcyanobiphenyl (8CB) with different silica arrangements providing the QRD. This LC provides a first-order isotropic to nematic (I-N) and second-order nematic to smectic-A (N-SmA) phase transition for the study of QRD.

There are three silica systems that are the focus of this paper: a colloidal gel of aerosil particles dispersed in the liquid crystal (denoted as 8CB+aerosil), a fused silica gel of aerogels immersed in 8CB (denoted as 8CB+aerogel), and a randomly interconnected controlled porous glass filled with 8CB (8CB+CPG). The LC+aerosil and LC+aerogel are nearly identical in every respect – fractal-like nature of the gel structure, surface chemistry, and density – save for their relative elasticity. Additionally, the ease of achieving nearly arbitrary silica densities for the aerosil system allows for greater control of the disorder. For the 8CB+aerosil system, thermal evidence for two regimes of behavior has been found [3]: low-density gels where pseudocritical behavior is closely related to that for the pure LC and higher-density gels where all transition features appear to be smeared. More rigid aerogels in LC+aerogel systems are crudely like the LC+aerosil gels in the high density regime but differ in some important ways since the elastic strain imposed by the random anchoring surfaces of aerogels is fully quenched. The LC+CPG has a topologically distinct arrangement of silica surfaces than either LC+aerogels or LC+aerosils (pores rather than voids), which varies the randomness of the fully quenched disorder. It appears that the disorder introduced by an aerogel is the greatest (all "transition" features are dramatically smeared) while that of CPGs is less so, and the physics of such systems may be more closely related to static random-elastic strain disorder.

The goal of this review is to catalog the thermodynamic results of phase transitions for the same liquid-crystal (8CB) interacting with the same surface (silicon-oxide) for three distinct random arrangements (fused gel, elastic gel, and porous glass) in order to sharpen the focus on the nature of quenched random disorder. It is organized as follows. A phenomenological description of gels and porous media are given in Sec. II. Section III reviews the essential behavior of the first-order isotropic to nematic (I-N) and the second-order nematic to smectic-A (N-SmA) transitions of the liquid crystal 8CB within three types of silica media; aerosil gels, aerogels, and controlled-porous glasses (CPGs) behavior near the N-SmA transition. The application of scaling analysis to calorimetric results on the 8CB+aerosil system is presented in Sec. IV with comparisons made to the 8CB+aerogel and 8CB+CPG systems. Section V summarizes the conclusions that can be drawn regarding the nature of quenched, randomness, and strength of the quenched-random disorder.

II. GENERAL DESCRIPTION OF POROUS MEDIA: RANDOM-SURFACE MODEL

For liquid-crystals, the introduction of quenched random disorder requires the inclusion of fixed random solid surfaces. This can be accomplished by the percolation of a low-volume-fraction gel structure randomly arranged throughout the LC host. Such gels can be physically realized by a diffusion-limited-aggregation or polymerization process, which forms fractal-like structures having a wide distribution of void length scales. In practical terms, the fractal-like character is limited to length scales much larger than the size of the basic unit and smaller than some macroscopic size limiting the gel, i.e., the sample size. These systems are typified by colloidal dispersions of silica within an LC host such as LC+aerosils and LC+aerogels.

Because of the hydroxyl groups on the surface of the 7 nm-diam hydrophilic aerosil (SiO_2) spheres used in this work, hydrogen bonding is possible between aerosil particles [22]. When dispersed in an organic liquid medium, aerosil particles comprising three to four lightly fused spheres and having a mean radius of gyration of ≈ 24 nm [3] will attach to each other and form a gel by a diffusion-limited aggregation process. This gel can be thought of as a randomly crossing "pearl necklace" of silica and a cartoon depiction is given in Fig. 1. The hydrogen-bonded nature of the silica "links" is relatively weak and gives these gels the ability to break easily and reform on moderate time scales (such gels are termed thixotropic). In addition, because of the diffusion-limited aggregation process by which gelation occurs, the structure of the final gel may become anisotropic if the gelation occurs in an anisotropic fluid, i.e., gelation in a well-aligned nematic or smectic liquid crystal. This gives such colloidal gels very attractive uses in future research as a route to studying anisotropic random disorder [23].

These aerosil gels are very similar in structure to the well-known and previously studied aerogels, which are another type of fractal silica gel. Aerogels are formed by a reaction-limited aggregation process and form a gel nearly identical to that of aerosils except that the nearly identical basic silica units in aerogels are chemically fused together. Thus, aerogels have a large shear modulus (they break before yielding) while in contrast aerosil gels have a quite small, density-dependent, shear modulus [24]. Thus, aerosil gels can respond elastically to strains, which may turn out to be a crucial difference as will be discussed later. For the

present work, the thixotropic character ensures that the silica strands mainly dictate, at low silica concentrations, the local nematic director without imposing high-energy elastic strains over the material throughout the void. As the silica density increases, the aerosil gel eventually becomes stiff enough to elastically strain the host fluid.

Another route is the inclusion of the LC within random porous media. Such a media is formed by the spinoidal decomposition of a binary glass melt then subsequent leaching of one of the glass components. These are widely known as controlled porous glasses (CPGs) or Vycor. The random solid surfaces in CPGs are topologically distinct from gels. In general, gels are random stands of nearly constant diameter, thus a solid chord length is a measure of the correlation of the surfaces. In CPGs, there is a direction where travelling along the solid surface returns to the starting point thus defining a pore circumference. See Fig. 2. An important difference between gels and CPGs is that gels have nearly identical base units thus the mean length of a solid region is nearly constant while for CPGs, the mean length of a solid depends strongly on silica density.

For any random arrangement of surfaces, a mean distance between solid surfaces or a mean open length, l_o, can be uniquely defined despite the wide distribution, this is denoted as a random-surface (RS) model. The definition of l_o in terms of macroscopic, and experimentally accessible, quantities begins by imagining a "straw" of uniform cross section A sent through the gel; see Fig. 1. The places where the gel randomly intersects the "straw" defines a solid length d_S while the distance between intersections defines a open length. The relevant macroscopic quantities are the specific surface area a in total surface area per mass (given as 300 $\mathrm{m}^2\ \mathrm{g}^{-1}$ [22] for the type R300 aerosil) and the conjugate density, ρ_S = mass of solid per open volume or in our case grams of silica per cm^3 of LC. Since the cross section of this imaginary straw is uniform, the proper summing of the total open and solid volumes of the straw depends only on the open and solid lengths, respectively, noting that each void must be bounded by two walls. The sum of the total solid length and the total open length is simply the length of the straw which spans the sample.

The two requirements for volume and length defined above allow the definition of the average open length as

$$l_o = 2/a\rho_S \ . \tag{1}$$

See Refs. [3] and [25] for a more detailed derivation. This definition of l_o is valid only in the dilute regime where the addition of more solid does not significantly change the

specific surface area. However, as the concentration of solid increases, more surface area is lost due to multiple connections ("clumping" of basic units); thus the specific surface area should be a decreasing function of the solid volume fraction Φ. A limiting case of interest is when completely enclosed pores occur. Here, the open volume is now bounded on all sides and a rederivation of the mean void (now pore) size along the lines described above yields $l_o = 6/a\rho_S$. This can be recast into the form given in Eq. (1) if $a_{\text{pore}} \rightarrow a_{\text{void}}/3$. Thus, Eq. (1) is a general for a random surface structure if the variation of a with ρ_S is known. The exact variation of a with solid concentration depends on the specific process of densification for gels and the kinetics of the spinoidal decomposition for CPGs. For gels, both aerosil gels and aerogels have nearly identical structures [16] and an estimate for the variation of $a(\rho_S)$, in m^2 per gram, is $a = 300 - 103.8\rho_S$, where ρ_S has the units grams of SiO_2 per cm^3 of LC. The condition for *completely closed pores* is crudely predicted to occur at $\rho_S \approx 1.97$ g cm^{-3} (assuming a continuous process of diffusion-limited aggregation). For all LC+aerosil and LC+aerogel samples studied to date, the density of silica employed has been well below that limit and the use of this estimate of $a(\rho_S)$ in Eq. (1) reproduces quite closely the SAXS measured void sizes of aerogels. For CPGs, this model does not work as well given that the first-order approximation of $a(\rho_S)$ is too crude as well as a mean-solid chord length strongly dependent on silica density. However, the mean-open length l_o and the specific surface area a are experimentally measurable by BET nitrogen isotherms and a test of this model (where the relation $a(\rho_S)$ has been used to eliminate ρ_S from Eq. (1) is shown in Fig. 3. This indicates some confidence in the general model, revealing a cross over from voids to pores at $a_c \sim a_o/2$, where a_o is the dilute regime specific surface area. The above considerations indicate that the mean-open length l_o can be used as a metric to compare the different CPGs and gels systems.

From the above discussion, the conjugate density ρ_S or l_o is an attractive quantity to describe the gel and its disordering character [26]. Note that the volume fraction of LC in a silica boundary layer of thickness l_b is given by $p = l_b a \rho_S$ [3]. This quantity p is the fraction of LC filling the voids that is in direct contact with the solid surfaces and thus considered strongly "pinned". Since p is a natural measure of the "disordering strength" of the gel, ρ_S is expected to be linearly related to this QRD strength for low to moderate ρ_S values [27].

III. GENERAL OBSERVATIONS OF 8CB+SILICA THERMODYNAMICS

A. First-order transitions with QRD: The isotropic to nematic transition

The isotropic to nematic behavior with the three type of QRD introduced by silica surfaces are characterized by two parameters: the total transition enthalpy ΔH_{IN} shown in Fig. 4 and the shift in T_{IN} shown in Fig. 5 as a function of l_o for 8CB+aerogel [16], 8CB+CPG [10], and 8CB+aerosil [3] (where available). There are two distinct behaviors. For 8CB+aerogel and 8CB+CPG samples, the $\Delta C_p(IN)$ behaves as a single feature, progressively broadening with increasing silica content or decreasing l_o. However, for 8CB+aerosil, a double $\Delta C_p(IN)$ feature is for silica content below $\rho_S \approx 0.1$ suggesting two transitions to the disordered nematic state while a single feature reminiscent of the 8CB+aerogel and 8CB+CPG samples is seen for higher densities. This two-regime behavior for the 8CB+aerosils is also reflected in the non-monotonic shift downward of T_{IN}. The total transition enthalpy also decreases with decreasing l_o for 8CB+CPG and 8CB+aerosil (the latent-heat was not measured for 8CB+aerogel samples) but below $l_o \approx 67$ nm, the 8CB+aerosil depresses ΔH_{IN} much more strongly. Both indicate that the first-order character decreases with decreasing l_o and consistent with the general behavior of first-order transitions with QRD [17] though there remains many questions regarding the details.

B. Second-order transitions with QRD: The nematic to smectic-A transition

Non-monotonic evolution of the effective transition temperature for the N-SmA transition is also seen and shown in Fig. 6 for 8CB+aerosils with comparison to 8CB+aerogel and 8CB+CPG systems (taken from the same references). The nematic temperature range shown in Fig. 7 indicate that for sufficiently small (large) ρ_S, the shift in T_{IN} and T^* track each other. For 8CB+aerogel and 8CB+CPG samples, the nematic range almost immediately begins to grow with decreasing l_o but over the thermodynamically sharp behavior of 8CB+aerosil it does not. The essential feature of $\Delta C_p(NA)$ is the observation that low silica density for 8CB+aerosil and for the 8CB+CPG samples pseudocritical behavior is found that parallels the critical behavior exhibited by pure LCs in spite of the absence of long-range smectic order. Calorimetric data for 8CB+aerosils [3] support this view that effective critical behavior occurs for low silica density 8CB+aerosil samples while a critical

analysis is still possible for 8CB+CPG samples [10].

The full power-law form in terms of the reduced temperature $t = \mid T - T^* \mid / T^*$ used to analyze experimental specific heat data associated with the N-SmA phase transition is [28]

$$\begin{aligned} \Delta C_p(NA) &= C_p(\text{observed}) - \text{C}_\text{p}(\text{background}) \\ &= A^{\pm} t^{-\alpha}(1 + D^{\pm} t^{\Delta_1}) + B_c \ , \end{aligned} \tag{2}$$

where the critical behavior as a function of reduced temperature t is characterized by an exponent α, an amplitude $A^{\pm}$ above and below the transition, a critical background term B_c, and corrections-to-scaling terms characterized by the coefficients $D^{\pm}$ and exponent $\Delta_1 \simeq 0.5$. The effective exponent α results for fits to the excess N-SmA specific-heat (heat capacity per gram of LC) data for 8CB+aerosil [3] and 8CB+CPG [10] as a function of inverse l_o (in order to capture the bulk behavior) is reproduced in Fig. 9. The results suggest that despite the difference in the topology of the surfaces (the randomness of the disorder), the evolution of the critical behavior is quite similar. Note that fits to the data with Eq. (2) can include only data for $\mid t \mid > \mid t_m^{\pm} \mid$ since the ΔC_p peak is truncated at a finite maximum value $h_M \equiv \Delta C_p^{\max}(NA)$.

IV. SCALING ANALYSIS OF THE *N*-SM*A* TRANSITION

In order to utilize a scaling analysis on second-order phase transitions, the maximum length scale ξ_M and the appropriate critical fluctuation parameters must be well characterized. While ξ_M may be directly measured as the saturated correlation length, it can also be inferred from the confining or disorder length scale. The critical fluctuation parameters are particularly well determined by calorimetric studies. Thus relevant scaling relations, described in detail in Ref. [29] are

$$\delta T^*/T^* \approx 2t_m^{+} = 2(\xi_M/\xi_{\|o})^{-1/\nu_\|}, \tag{3}$$

$$h_M = A^{\pm}(\xi_M/\xi_{\|o})^{\alpha/\nu_\|}[1 + D^{\pm}(\xi_M/\xi_{\|o})^{-\Delta_1/\nu_\|}] + B_c \ , \tag{4}$$

to describe the fractional temperature rounding of the transition and the specific-heat maximum, respectively. Here, two approximations will be explored. In the first case, the mean void size (or disorder length scale) is used as the cutoff length scale $\xi_M = l_o$ and the *bulk* critical parameters. This approach represents conventional finite-size scaling, denoted as

FSS, where the cut off length scale is set by a natural length of the "confinement." In the second case, the calorimetrically determined critical parameters and two-scale predictions for the bare correlation length and exponent are used to set the cutoff length scale to the saturated (low-temperature) parallel smectic correlation length, i.e., $\xi_M = \xi_{\parallel}^{\mathrm{LT}}$. This analysis recognizes that the random-field effects truncate the growth of order and tests whether two-scale universality is obeyed on approaching this truncation. This approach is labelled random-field scaling, or RFS for short.

The specific-heat maximum $h_M \equiv \Delta C_p^{\max}(NA)$ is plotted versus ρ_S in Fig. 10 for 8CB+aerogel, 8CB+CPG, and 8CB+aerogel samples. Given as the solid line on this log-log plot is the simple scaling prediction using only the leading singularity of the pure 8CB heat capacity and the l_o as the truncation length. Interestingly, the full FSS analysis, which uses the pure 8CB critical parameters and $\xi_M = l_o$ from Eq. (1), appears to work very well over the entire range of l_o for the 8CB+aerosil system. This is surprising since the critical behavior of the 8CB+aerosil samples is changing with silica content, see Ref. [3] the saturated parallel smectic correlation length $\xi_{\parallel}^{\mathrm{LT}}$ is much larger than l_o for all samples [15]. Thus, the significance of this agreement is not clear. Both the 8CB+aerogel and 8CB+CPG scaling follow a simple l_o^{-1} relation not contained by the FSS analysis.

The analysis denoted as RFS uses the evolving specific heat critical behavior and two-scale universality predictions for the equivalent correlation length critical behavior for at each ρ_S for the 8CB+aerosil samples. The low-temperature experimentally measured saturated parallel correlation length $\xi_{\parallel}^{\mathrm{LT}}$ [15] is used as the truncation length ξ_M. This analysis reproduces very closely the observed heat capacity maximum and is completely consistent with both the effective critical behavior and the maximum smectic correlation length. Unfortunately, this analysis is only applicable up to $\rho_S \approx 0.1$, or $l_o > 67$ nm, since a critical analysis of $\Delta C_p(NA)$ is not possible for larger ρ_S [3]. Note that h_M for 8CB+aerogel samples cannot be described by either scaling methods. For either scaling approximation to reproduce the aerogel results, a far smaller ξ_M is required indicating that the aerogel has a much stronger disordering influence than the aerosil at any given ρ_S value. No saturated low-temperature smectic correlation lengths are available for 8CB+CPG but given the similarity of the critical evolution between 8CB+aerosil and 8CB+CPG, these too would have to be quite small.

The fractional rounding of the transition $\delta T^*/T^*$ for 8CB+aerosil and 8CB+aerogel sam-

ples is given versus ρ_S in Fig. 11. For samples where critical specific-heat fits were not possible, i.e., 8CB+aerosil for $\rho_S > 0.1$ and all 8CB+aerogel samples, the fractional rounding is estimated ad hoc as $\approx 10\%$ larger than the width between inflection points in ΔC_p. As was seen in Fig. 10, the FSS analysis works well for *all* densities of 8CB+aerosil samples. As before, this is surprising given the known changes in critical behavior and the fact that $\xi_{\parallel}^{\mathrm{LT}} > l_o$. The RFS analysis predicts a somewhat sharper transition than is observed. The observed rounding is not likely influenced by the amplitude of temperature oscillations employed by the ac-calorimetric technique in Refs. [3] and [16], which is on the order of 5 mK and would account for a fractional rounding of only $\sim 10^{-5}$. The estimation $t_m^- = t_m^+$ explicit in Eq. (3) may be in question as it assumes that the unknown critical behavior of the correlation length below T^* is the same as that above T^*. A consequence of these arguments is that the agreement of FSS is likely accidental although intriguing. Again, the 8CB+aerogel and 8CB+CPG fractional rounding is much larger than that for the 8CB+aerosil samples, which is an indication that a smaller ξ_M is required and supports the view of a stronger disordering influence for the aerogel than the aerosil.

Figure 8 presents the N-SmA transition enthalpy δH_{NA} versus ρ_S for 8CB+aerosil and 8CB+aerogel samples. Unlike h_M and $\delta T^*/T^*$ which are measures of truncation effects on ΔC_p very close to T^*, $\delta H_{NA} = \int \Delta C_p(NA)dT$ is sensitive to both truncation and changes in the shape of ΔC_p over its entire temperature range. This is discussed in detail in Ref. [3]. A finite-size scaling analysis for δH_{NA} proceeds by integrating the available ΔC_p critical form approximately ± 3 K about T^* ($|t| \approx 10^{-2}$) to the point corresponding to $t_m^{\pm}$. As an approximation, a linear evolution of ΔC_p between t_m^+ and t_m^- is assumed. The FSS analysis, given by the solid line in Fig. 8, does not agree well with the data for either system. The failure of this model is not surprising since it ignores any changes in the ΔC_p critical parameters such as $A^{\pm}$ and α with ρ_S. A RFS analysis would not be very meaningful for δH_{NA} since for $\rho_S < 0.1$, the input parameters for this model automatically ensure perfect agreement. Also, the necessary input critical parameters cannot be obtained for 8CB+aerosil samples with $\rho_S > 0.1$ or for any of the 8CB+aerogel samples.

V. DISCUSSION AND CONCLUSIONS

Despite the loss of long-range smectic order, quasicritical thermal fluctuations remain important at high temperatures for low silica density 8CB+aerosil and 8CB+CPG samples. In addition, two-scale universality analysis provides a link between the SmA quasicritical behavior of the heat capacity and the correlation lengths. The smectic fluctuations are modified from the pure 8CB behavior due to the effects of quenched random disorder. The evolution of the effective critical exponent α for the 8CB+aerosil and 8CB+CPG systems as a function of l_o mirrors that of pure LCs as a function of the McMillan ratio R_M reflecting the suppression of the nematic susceptibility with increasing nematic temperature range. As shown in Ref. [15], the density ρ_S of an aerosil gel is directly correlated to the McMillan ratio R_M of pure LCs, both of which are indicators of the strength of smectic-nematic coupling. The flow of the effective critical behavior for the N-SmA transition shown in Fig. 9 as a function of QRD induced decoupling is consistent with theoretical predictions that no new fixed point is present for the RFXY model [13]. For the liquid-crystal – silica dispersion system studied here, the flow is from near a Gaussian tricritical point toward the 3D-XY fixed point and appears independent of the topology of the silica structure.

This crossover behavior is explained for pure LCs by a decrease in nematic – smectic coupling as R_M decreases. For 8CB+aerosils, an increase in ρ_S appears to have the same effect. Recent work has found that aerosil gels exhibit dynamics which can couple to a host liquid crystal [30] presumably through direct coupling to director fluctuations. Also, recent deuterium NMR studies of 8CB+aerosils [6] found no appreciable change in the magnitude of orientational order above T^* for $\rho_S < 0.1$. The reason appears to be that the aerosil particles form a hydrogen-bonded thixotropic 3D gel network that provides (a) random anchoring surfaces for 8CB molecules and (b) because of the flexible/fragile nature of the silica gel, random elastic dampening of elastic (director) fluctuations occurs in the liquid crystal. Both effects will reduce the nematic orientational susceptibility by suppressing *director* fluctuations. Thus, increasing ρ_S in LC+aerosil samples is equivalent to decreasing R_M in a pure liquid crystal, which in the case of 8CB drives its critical behavior towards XY. This may have important consequences for the *bulk* N-SmA behavior as theoretical efforts have mostly concentrated on the de Gennes type of smectic coupling to the magnitude of nematic order, and it appears that the coupling to director fluctuations may play an

important role in this crossover behavior.

Because the random disorder is introduced by the inclusion of network gel structures within the liquid crystal, finite-size effects can exist and may play a role in truncating thermally driven fluctuations. Such effects would explain the increasing suppression of the heat capacity peak with increasing ρ_S, which corresponds to decreasing the mean distance between solid surfaces. Scaling analysis provides a good description of the maximum heat capacity and the fractional rounding (or truncation) of the transition for all 8CB+aerosil samples. However, FSS analysis does not provide a good prediction of the trend with ρ_S for the transition enthalpy $\delta H_{NA} = \int \Delta C_p(NA)dT$. The reason for this is the fact that the trend in δH_{NA} is dominated not by the truncation of the $\Delta C_p(NA)$ peak but by the changes in shape and size of $\Delta C_p(NA)$ over its entire range, and the latter effect is due to crossover rather than finite size.

Below the pseudotransition temperature T^*, the correlation lengths and the amplitudes of the thermal term in the smectic structure factor for 8CB+aerosils saturate and are approximately temperature-independent [15]. Quenched random disorder imposed by the aerosil gel network dominates the smectic fluctuations below the pseudotransition. The low-temperature parallel correlation lengths $\xi_{\parallel}^{\mathrm{LT}}$ taken from [15] plus the corresponding perpendicular $\xi_{\perp}^{\mathrm{LT}}$ values and the mean correlation lengths $\bar{\xi} = (\xi_{\parallel}\xi_{\perp}^2)^{1/3}$. Also plotted are the "isotropic" smectic correlation lengths reported at low temperature for 8CB+aerogel samples [4], the mean-open length l_o based on Eq. (1), and an estimate of the saturated *nematic director* correlation length ξ_N measured in 6CB+aerosil samples [5]. The parallel correlation length is much larger than l_o but smaller than ξ_N for all 8CB+aerosil samples studied. The first fact indicates than the smectic domains span many "voids" and it is thus reasonable to expect that their influence is of a random-field type, while the latter fact is physically reasonable since the observed smectic domains cannot be larger than the size of a nematic domain. However, 6CB does not exhibit a smectic phase, so it remains unknown how the director correlation length would change, if at all, due to the onset of smectic order. Interestingly, the low-temperature 8CB+aerogel correlation lengths appear to agree fairly well with l_o, while the aerogel $\Delta C_p(NA)$ peak is severely rounded, indicating that 8CB is very strongly perturbed by the rigid fused silica gel.

This idea of *two* regimes may be consistent with the picture of the aerosil gel described earlier where, in addition to the random silica strands ("pearl-necklace" of aerosil beads)

providing the random field dictating the local orientation of the nematic director, there perhaps exists an elastic coupling of these tenuous strands to the nematic director. This coupling would dampen the size of director fluctuations analogous to the effect of a wider nematic temperature range, and this gives a physical interpretation to the critical flow with random-field strength towards the underlying XY fixed point. The apparent increase in the *relative* effect of the elastic coupling seen by the stronger scaling of the quenched random disorder strength with silica density may be an indication that the aerosil gel has become significantly stiffer when $\rho_S > 0.1$, suggesting the possibility that a rigidity transition has occurred in the gel.

In conclusion, a combination of finite-size effects and two-scale universality concepts has yielded a successful connection between 8CB+aerosil thermal behavior and x-ray correlation length behavior. The truncation of $\Delta C_p(NA)$ peaks, measured by h_M and $\delta T^*/T^*$, and the observation of high-temperature 8CB+aerosil correlation lengths that are close to those for pure 8CB are both well explained. The observed dependence of the integrated area δH_{NA} on ρ_S is not properly described by finite-size scaling, and the reason for this failure is clear. Trends in $\delta H_{NA}(\rho_S)$ reflect the changing shape of ΔC_p peaks over a wide temperature range as ρ_S varies. As described in Ref. [15] and in Sec. IV of the present paper, quenched random disorder plays a dominant role in changing the effective pseudocritical exponents that describe the smectic behavior in 8CB+aerosils. Such scaling relations do not work for the nearly identical 8CB+aerogel system nor the topologically distinct 8CB+CPG system. It seems possible that the elasticity of the aerosil gel plays an important part in the theory of gels as a random perturbation acting on the N-SmA transition in liquid crystals. Theory incorporating such elastic aspects is in progress [19]. The decoupling of nematic and smectic order parameters may also occur in a highly interconnected porous structure of 8CB+CPG via the pore geometry directly suppressing director fluctuations and may be understood in view of a *single-pore* model [10].

Acknowledgments

I am indebted to A. Roshi, C. W. Garland, R. L. Leheny, S. Park, P. Clegg, T. Bellini, L. Radzihovsky, N. A. Clark, T. Bellini, and A. Aharony for many helpful discussions. This

work was supported by the NSF under the NSF-CAREER award DMR-0092786 (WPI).

---

[1] M. Chan, N. Mulders, and J. Reppy, Physics Today **49**, 30 (1996), and references therein.

[2] Q. J. Harris, Q. Feng, Y. S. Lee, R. J. Birgeneau, and A. Ito, Phys. Rev. Lett. **78**, 346 (1997), and references therein.

[3] G. S. Iannacchione, C. W. Garland, J. T. Mang, and T. P. Rieker, Phys. Rev. E **58**, 5966 (1998).

[4] T. Bellini, L. Radzihovsky, J. Toner, and N. A. Clark, Science **294**, 1074 (2001).

[5] T. Bellini, N. A. Clark, V. Degiorgio, F. Mantegazza, and G. Natale, Phys. Rev. E **57**, 2996 (1998).

[6] T. Jin and D. Finotello, Phys. Rev. Lett. **86**, 818 (2001).

[7] B. Zhou, G. S. Iannacchione, C. W. Garland, and T. Bellini, Phys. Rev. E **55**, 2962 (1997).

[8] M. Marinelli, A. K. Ghosh, and F. Mercuri, Phys. Rev. E **63**, 061713 (2001).

[9] S. Park, R. L. Leheny, R. J. Birgeneau, J.-L. Gallani, C. W. Garland, and G. S. Iannacchione, Phys. Rev. E **65**, 050703(R) (2002).

[10] Z. Kutnjak, S. Kralj, G. Lahajnar, and S. Žumer, Fluid Phase Equilibria (2003), submitted.

[11] G. S. Iannacchione, G. P. Crawford, S. Qian, J. W. Doane, D. Finotello, and S. Zumer, Phys. Rev. E **53**, 2402 (1996).

[12] G. S. Iannacchione, S. Qian, D. Finotello, and F. M. Aliev, Phys. Rev. E **56**, 554 (1997).

[13] A. Pelissetto and E. Vicari, Phys. Rev. B **62**, 6393 (2000).

[14] L. Radzihovsky and J. Toner, Phys. Rev. B **60**, 206 (1999).

[15] R. L. Leheny, S. Park, R. J. Birgeneau, J.-L. Gallani, C. W. Garland, and G. S. Iannacchione, Phys. Rev. E (2002), preceding paper, denoted as paper I.

[16] L. Wu, B. Zhou, C. W. Garland, T. Bellini, and D. W. Schaefer, Phys. Rev. E **51**, 2157 (1995).

[17] Y. Imry and M. Wortis, Phys. Rev. B **19**, 3580 (1979).

[18] D. E. Feldman, Phys. Rev. Lett. **84**, 4886 (2000).

[19] L. Radzihovsky, private communications.

[20] P. D. Olmsted and E. M. Terentjev, Phys. Rev. E **53**, 2444 (1996).

[21] S. P. Meeker, W. C. K. Poon, J. Crain, and E. M. Terentjev, Phys. Rev. E **61**, R6083 (2000).

[22] Degussa Corp., Silica Division, 65 Challenger Road, Ridgefield Park, NJ 07660. Technical data

given in the Degussa booklet AEROSILS.

[23] R. Leheny, D. Liang, A. Roshi, and G. Iannacchione, unpublished.

[24] H. Sonntag and K. Strenge, *Coagulation Kinetics and Structure Formation* (Plenum Press, New York, 1987), pp. 134–145 and 172–177.

[25] G. Porod, *Small Angle X-ray Scattering* (Academic Press, London, 1982), chap. 2, pp. 18–51, eds. O Glatter and O Kratky.

[26] Together with the overall density of solid, $\rho =$ mass of solid per total sample volume, and the density of the solid itself, $\rho_M =$ mass of solid per solid volume (2.2 g cm^{-3} for silica) where $\rho^{-1} = \rho_S^{-1} + \rho_M^{-1}$, other gel parameters may be determined. Note that as ρ varies from zero (no solids present) to its maximum of ρ_M (all solids, no open volume), ρ_S varies from zero ($l_o \to \infty$, or sample size) to infinity ($l_o \to 0$, or no open volume). The solid volume fraction is given by $\Phi = \rho/\rho_M$ while the open volume fraction, or porosity, is given by $\phi = 1 - \Phi = \rho/\rho_S$.

[27] Note that only over some, as yet not well defined, range of solids concentration can an increase in Φ be considered an increase in the "strength" of the quenched disorder. In reality, the surface interactions between the material filling the voids and the solid surfaces are dictated by the materials themselves and remain constant. Since liquid crystals are quite "soft" materials elastically, the quenched state of molecules at a surface decays relatively slowly away from the surface. Thus, a point will occur where p $<$ 1 and yet everything between the surfaces can be considered quenched. In general, increasing Φ for large values of Φ only increases the extent of the surfaces and so the extent of the disorder but not its strength.

[28] C. W. Garland and G. Nounesis, Phys. Rev. E **49**, 2964 (1994).

[29] G. S. Iannacchione, S. Park, C. W. Garland, R. J. Birgeneau, and R. L. Leheny, Phys. Rev. E (2002).

[30] C. C. Retsch, I. McNulty, and G. S. Iannacchione, Phys. Rev. E **65**, 032701 (2002).

[31] A. Aharony, private communications.

[32] CPG, Inc., 3 Borinski Road, Lincoln Park, NJ 07035. Technical data given in http://www.cpg-biotech.com/cpgp/properties.html.

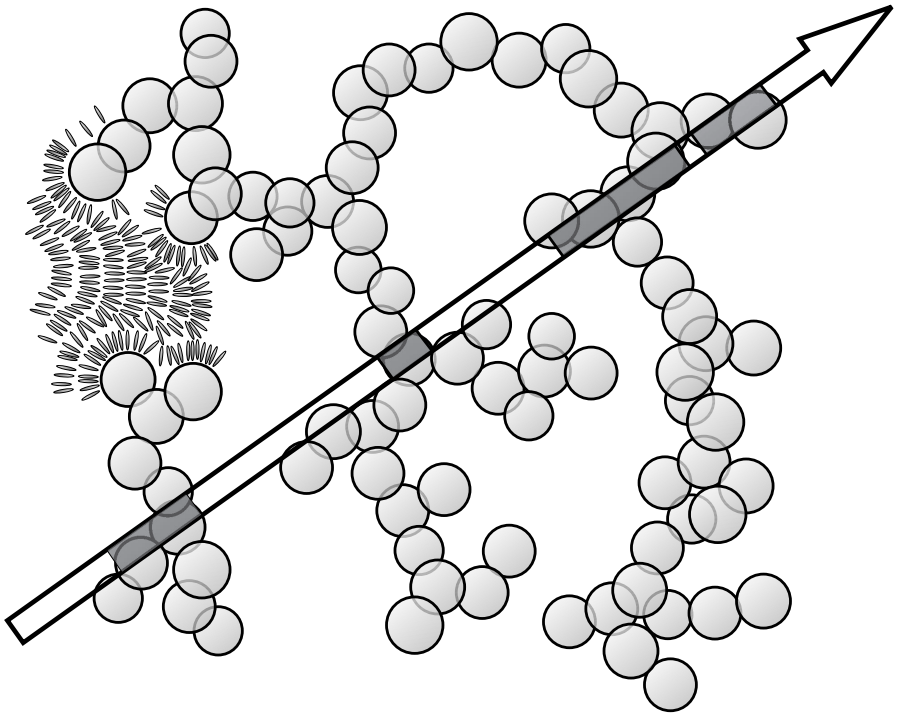

FIG. 1: A cartoon of an aerosil gel formed by a diffusion-limited-cluster aggregation process (a similar structure is seen for aerogels but formed by a DL-polymerization process, both DLCA and DLP yield fractal-like gels). Circles and "hairs" (upper left) represent type-300, 7-nm-diam, aerosil particles and 8CB molecules, respectively, drawn to approximate scale. This cartoon corresponds to an average open length $l_o \approx 40$ nm and $\rho_S \approx 0.20$, where the density units are grams of silica per cm^3 of 8CB. The solid volume fraction is $\Phi \approx 0.08$. Open and shaded parts of the arrow depict open and solid chords, respectively.

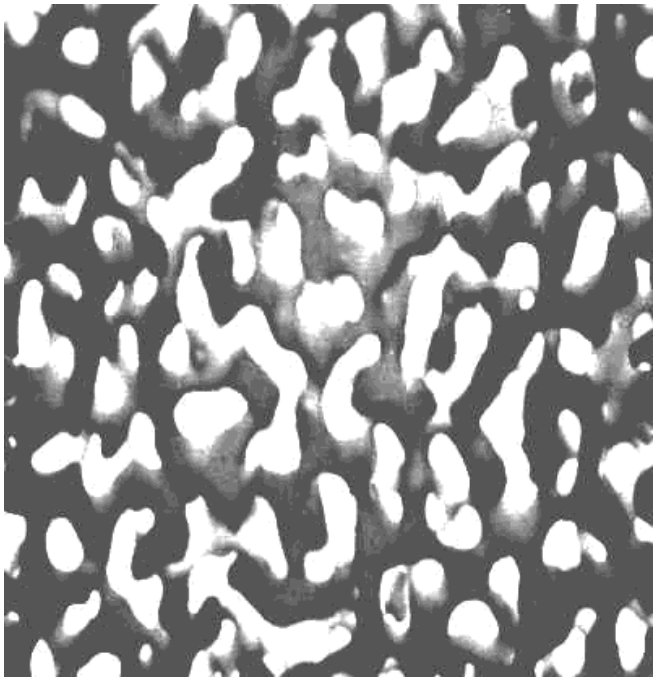

FIG. 2: A cartoon of a controlled porous glass formed by spinoidal decomposition of a binary glass melt. Note the presence of highly interconnected random pores rather than the topologically distinct voids of gels seen in Fig. 1. The fundamental difference arises from the mean-solid chord for porous media being strongly dependent on the specific surface area whereas in gels it is nearly constant.

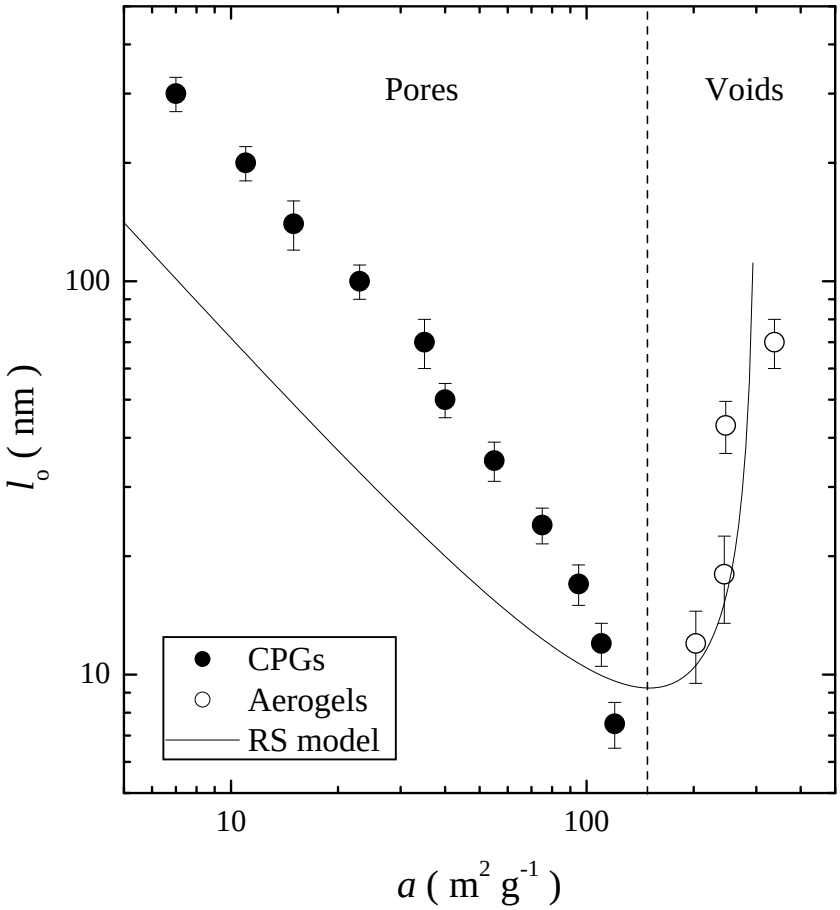

FIG. 3: Mean-open size (l_o) versus specific surface area (a) for controlled-porous glasses (determined by nitrogen isotherms [32]) and aerogels (determined by small-angle x-ray scattering [16]). The random-surface (RS) model (solid line) is also shown and connects l_o to a via the conjugate density ρ_S, see text. The vertical dashed line indicates the boundary between pores and voids, occurring at $a_c \sim a_o/2$.

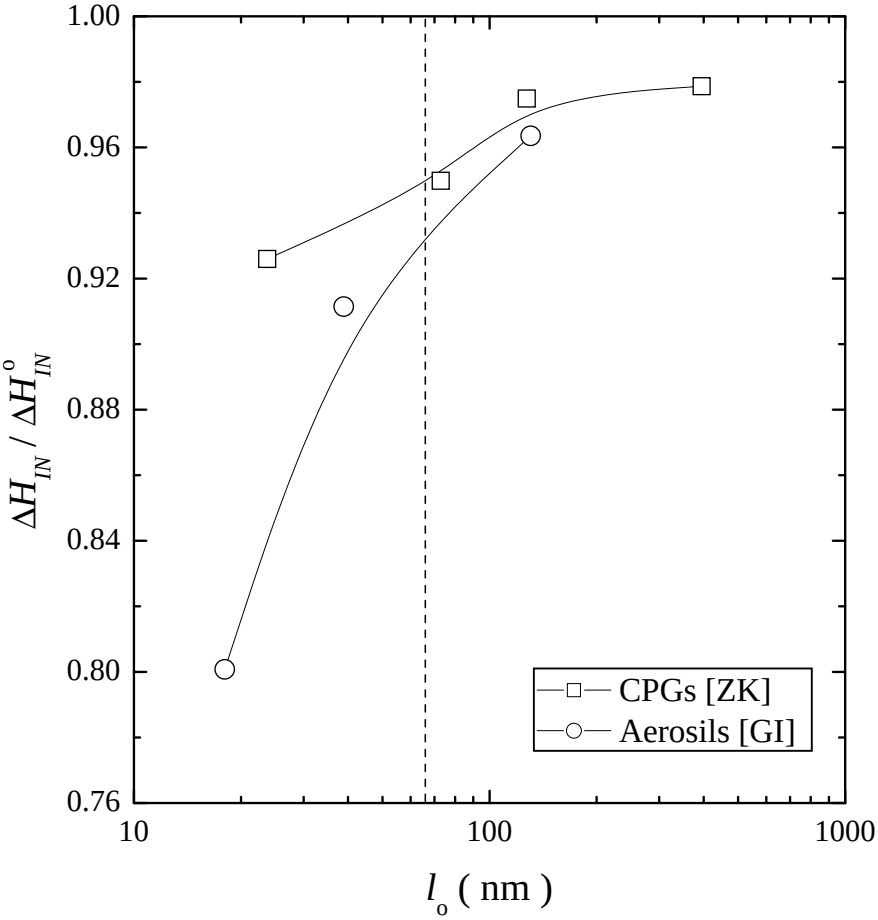

FIG. 4: A semi-log plot depicting the evolution of the total I-N transition enthalpy normalized to the bulk value ΔH^o_{IN} as a function of mean-open length l_o for 8CB+CPG [10] and 8CB+aerosil [3] systems. The vertical dashed line indicates the boundary between soft and stiff aerosil gels [3].

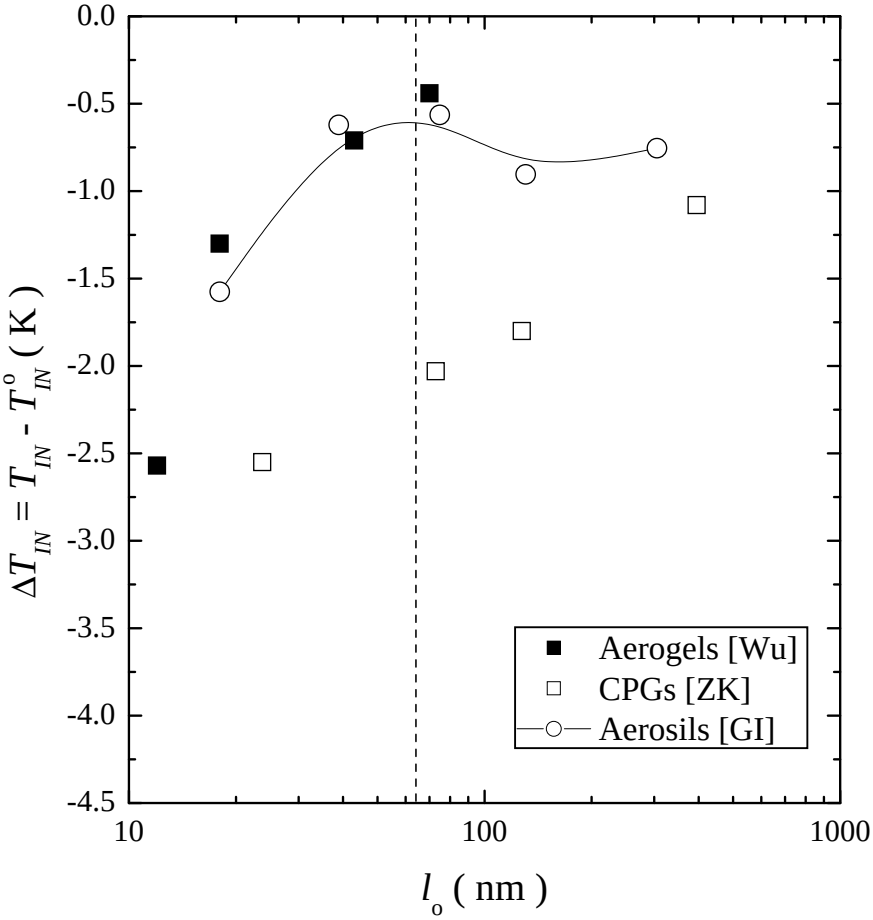

FIG. 5: A semi-log plot of the I-N transition temperature shift from the bulk transition temperature T^o_{IN} as a function of mean-open length for 8CB perturbed by aerogels [16], CPGs [10] and aerosils [3], see legend. The vertical dashed line indicates the boundary between soft and stiff aerosil gels [3].

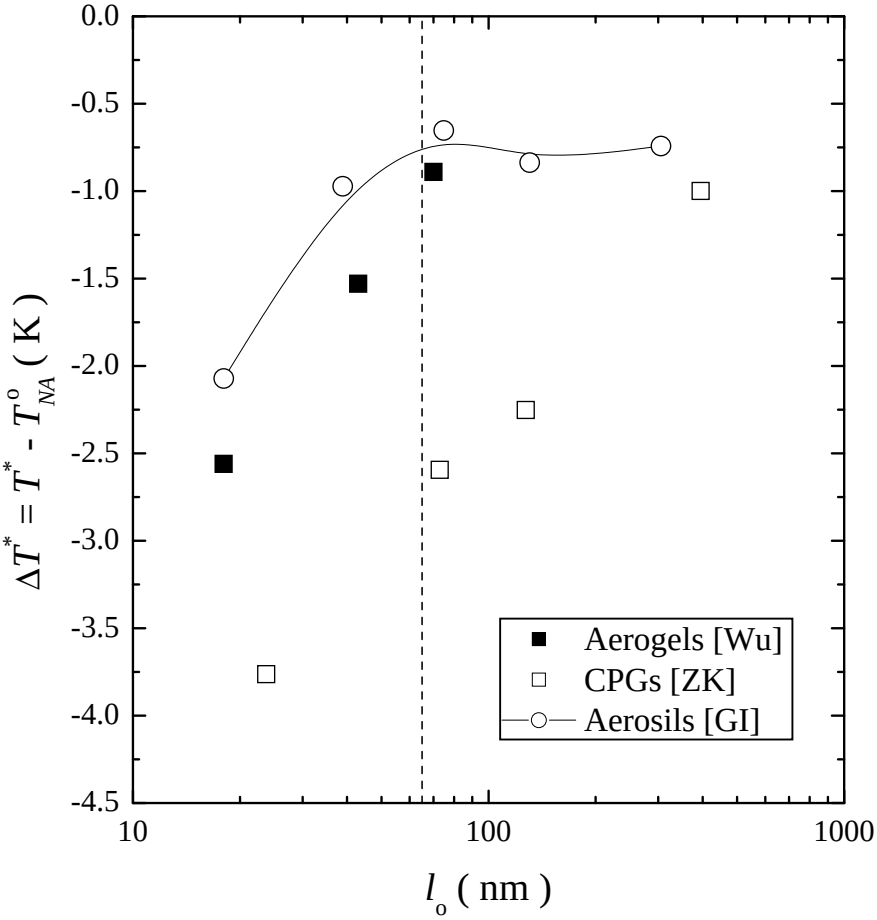

FIG. 6: The N-SmA transition temperature shift from the bulk transition temperature T^o_{NA} on a semi-log plot with the mean-open length for 8CB perturbed by aerogels [16], CPGs [10] and aerosils [3]. Note the generally larger shifts of the smectic phase boundary. The vertical dashed line indicates the boundary between soft and stiff aerosil gels [3].

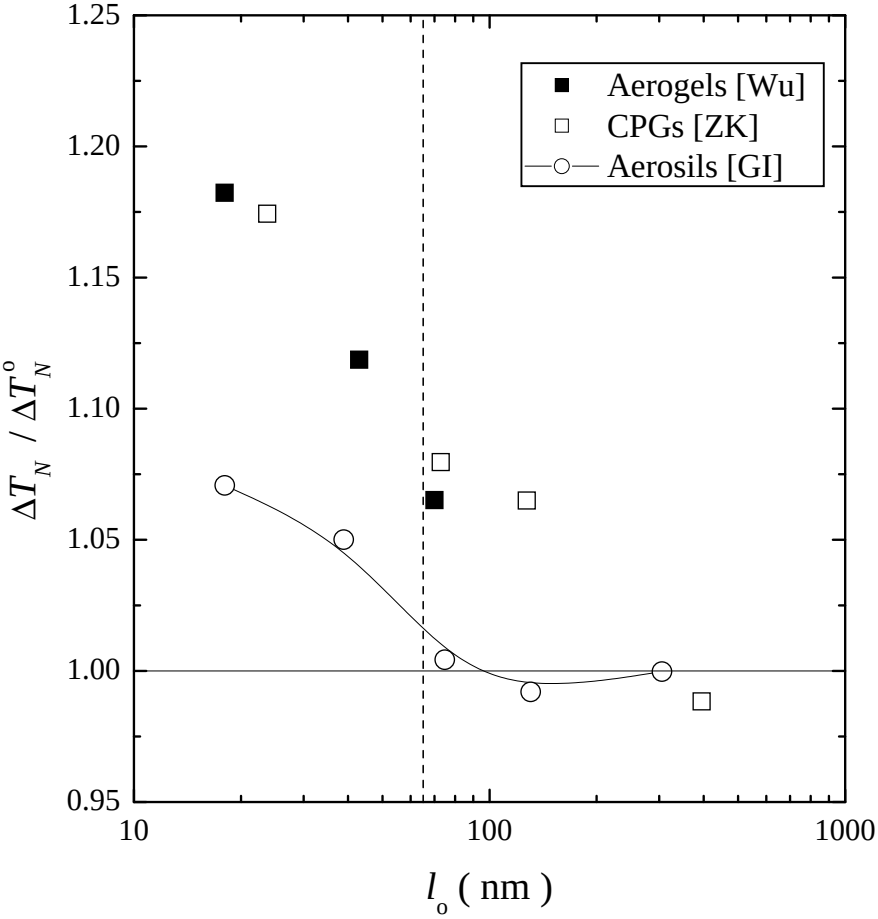

FIG. 7: A semi-log plot of the nematic temperature range scaled by the bulk value versus the mean-open length for 8CB+aerogel [16], 8CB+CPG [10] and 8CB+aerosil [3] systems. The vertical dashed line indicates the boundary between soft and stiff aerosil gels [3].

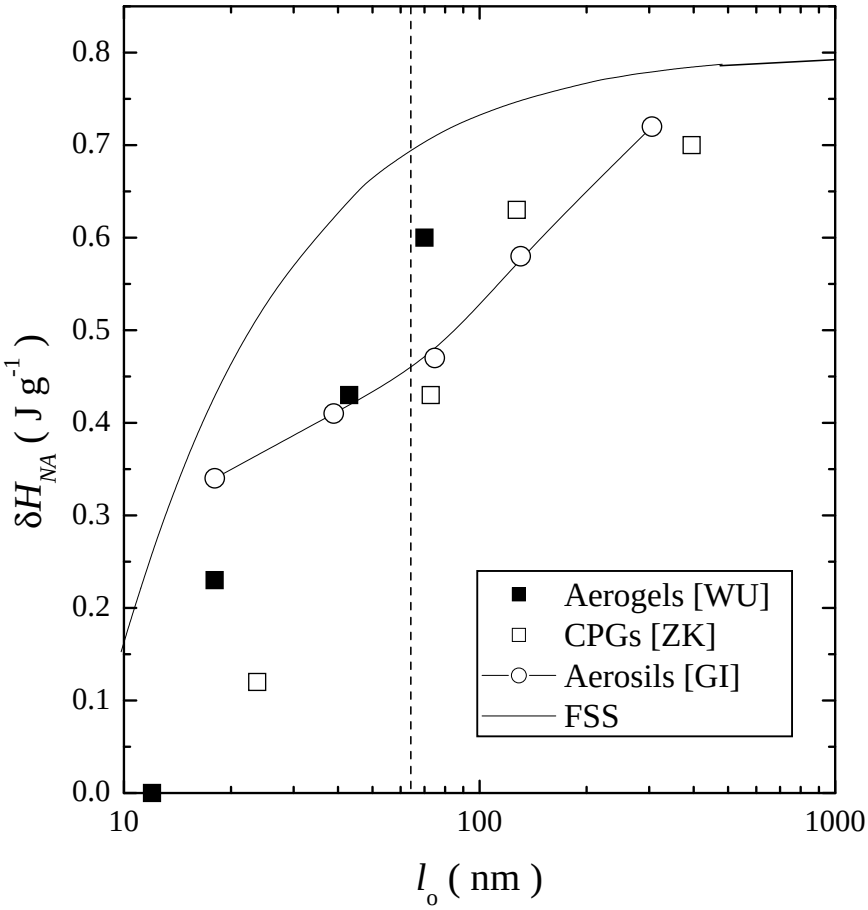

FIG. 8: The l_o dependence of the N-SmA transition enthalpy $\delta H_{NA} = \int \Delta C_p(NA)dT$ for 8CB perturbed by silica on a semi-log scale. As before, data taken from Ref. [16] for 8CB+aerogels, Ref. [10] for 8CB+CPGs, and Ref. [3] for 8CB+aerosils, see legend. The solid line depicts FSS using bulk 8CB critical parameters using $\xi_M = l_o$ while the vertical dashed line indicates the boundary between soft and stiff aerosil gels [3].

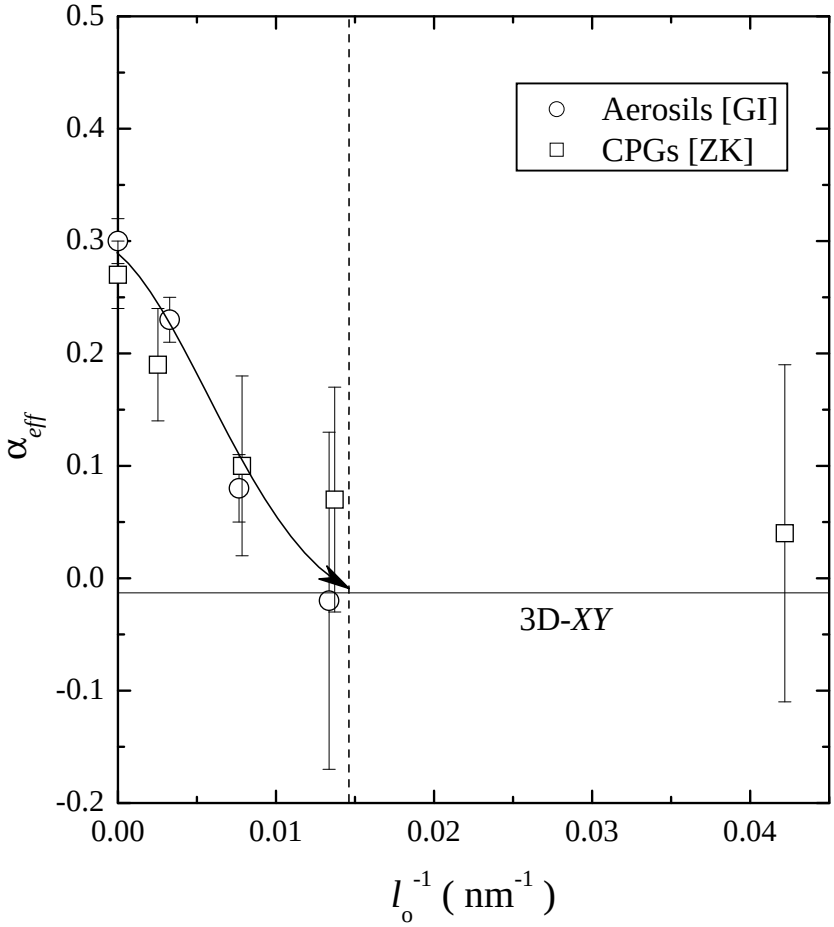

FIG. 9: The effective heat capacity critical exponent α obtained from Ref. [3] for 8CB+aerosils and Ref. [10] for 8CB+CPGs plotted against the inverse of the mean-open length (proportional to the conjugate silica density ρ_S, see text). Note the similar flows toward the underlying 3D-XY behavior with increasing QRD indicating similar suppression of nematic coupling between the two systems. The vertical dashed line indicates the boundary between soft and stiff aerosil gels [3].

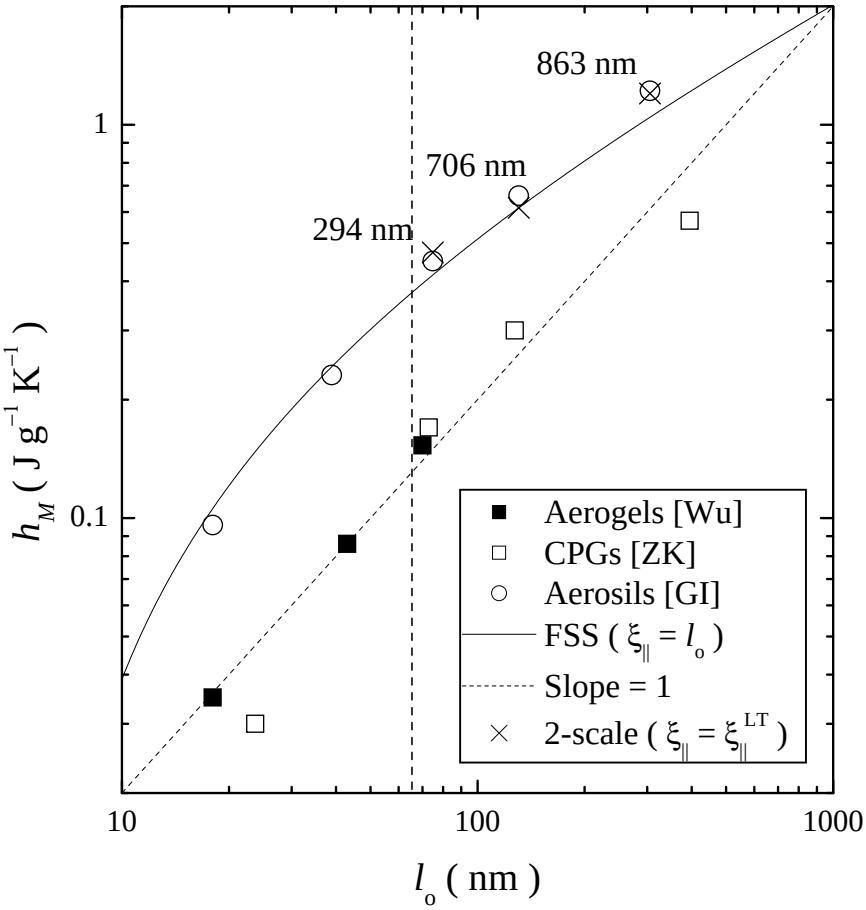

FIG. 10: Scaling plot of the N-SmA truncation $h_M \equiv \Delta C_p^{\max}(NA)$ versus l_o for 8CB+aerogel [16], 8CB+CPG [10], and 8CB+aerosil [3] systems. Both the solid line depicts FSS predictions based on using bulk 8CB critical parameters $\xi_{\|o}$ and $\nu_{\|}$ to find the reduced temperature where $\xi_M = l_o$ and includes corrections-to-scaling; see text. The dashed line indicates a slope of 1 common to both aerogel and CPG perturbations. The $\times$'s are based on a RFS analysis using two-scale predicted critical parameters (see text) and $\xi_M = \xi_{\|}^{LT}$ found in Ref. [15] (the values are noted in the figure).

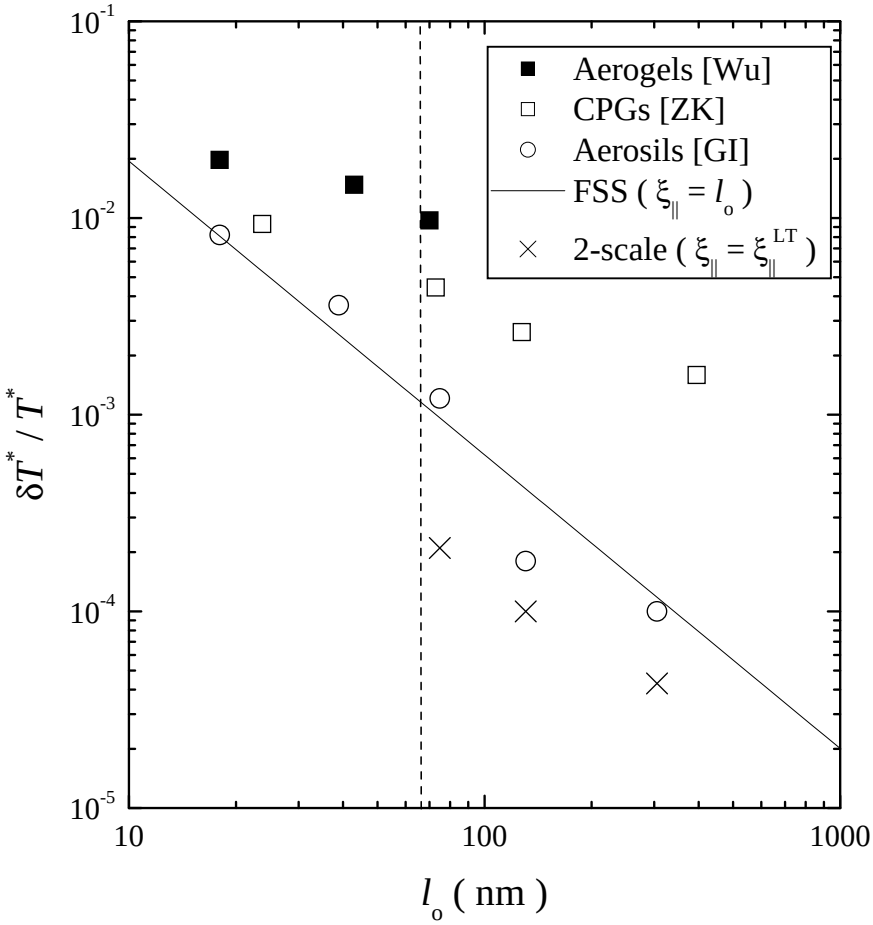

FIG. 11: A scaling plot of the fractional round-off region (gap about T^*) for the N-SmA transition where C_p power laws fail versus the mean-open length. The solid line depicts FSS predictions using bulk critical parameters and the fluctuation cut off length, $\xi_M = l_o$. The $\times$'s depict RFS predictions using two-scale critical parameters and $\xi_M = \xi_{\parallel}^{\mathrm{LT}}$ from Ref. [15].